Received: 6 June 2019 | Revised: 15 August 2019 | Accepted: 7 September 2019

DOI: 10.1002/aoc.5265

FULL PAPER

WILEY Applied Organometallic Chemistry

Binuclear and polymeric Hg(II) complexes of an ambidentate phosphorus ylide: Synthesis, crystal structure, antibacterial activity, and theoretical studies

Seyyed Javad Sabounchei[1] | **Faeze Kazemi Andalib**[1] | **Marjan Hosseinzadeh**[1] | **Asieh Sedghi**[1] | **Ali Hashemi**[1] | **Roya Karamian**[2] | **Kristof Van Hecke**[3]

[1] Faculty of Chemistry, Bu-Ali Sina University, Hamedan 65174, Iran

[2] Department of Biology, Faculty of Science, Bu-Ali Sina University, Hamedan 65174, Iran

[3] XStruct, Department of Chemistry, Ghent University, Krijgslaan 281-S3, B-9000 Ghent, Belgium

Correspondence
Seyyed Javad Sabounchei, Faculty of Chemistry, Bu-Ali Sina University, Hamedan, 65174, Iran.
Email: jsabounchei@yahoo.co.uk

The new α-keto-stabilized phosphorus ylide $Ph_3PCHC(O)PhCN$ (**Y**) was synthesized by addition of triphenylphosphine to 2-bromo-4′-cyanoacetophenone, followed by treatment with NaOH 10%. Reaction of ligand (**Y**) with methanolic solution of mercury(II) halides under mild conditions yielded the binuclear complexes $[Y{\cdot}HgX_2]_2$ [X=Cl (**1**), Br (**2**), I (**3**)]. The new organic/inorganic composite polymer $[Hg(NO_3)_2(Y)]_n$ (**4**) was synthesized by the reaction of mercury (II) nitrate with the phosphorus ylide **Y**. Compounds synthesized were characterized by Fourier-transform infrared, ^1H, ^{31}P, and ^{13}C nuclear magnetic resonance spectroscopic methods, which confirmed the coordination of ylide to the metal center through the ylidic carbon atom. Single-crystal X-ray structures of phosphorus ylide **Y** and polymeric complex **4** were also determined and the crystallographic data of complex **4** showed that the title complex has an infinite one-dimensional structure. Furthermore, the electronic and molecular structures of complexes **1–3** were investigated at the BP86/def2-SVP level of theory, indicating an increasing trend for C→M bond lengths: $Hg_2I_2 > Hg_2Br_2 > Hg_2Cl_2$ in $[Y{\rightarrow}HgX_2]_2$ (X = Cl, Br, I) complexes. In addition, the antibacterial activity of ligand **Y** and all complexes using the agar disc diffusion method was examined against both selected gram-positive and gram-negative bacteria. Results indicated that the ligand **Y** and complexes **1** and **4** show good antibacterial effect against gram-positive bacteria tested; besides, the inhibition zones of complexes were significantly larger than those of chloramphenicol as standard.

KEYWORDS

antibacterial activity, crystal structure, phosphorus ylide, spectroscopic characterization, theoretical studies

1 | INTRODUCTION

Organophosphorus compounds are important in synthetic organic chemistry, particularly in the synthesis of compounds with biological and pharmacological properties.[1–4] Phosphorus ylides, a special class of zwitterions, carry strongly nucleophilic electron-rich carbanions. The electron distribution around the $P^+–C^-$ bond and its resulting chemical implications have been explored and assessed through theoretical, spectroscopic, and crystallographic investigation. In recent years, multiple reports for the synthesis of new phosphorus ylides have been published which renders their study an outstanding conquest in the chemistry of the twentieth century.[5] They are usually prepared by the treatment of a phosphonium salt with a base. The corresponding phosphonium salts can be synthesized by Michael addition of phosphorus nucleophiles to the activated alkyl/aryl halides.[2,3,6] The chemistry of metal complexes with ylides is a subject of present interest.[7] The α-stabilized phosphorus ylides [$Ph_3P{=}C(H)R$] [R=CN, C(O)R′; R′ = Me, Ph, OMe, NMe_2] have proven to be versatile ligands toward transition metals because of the presence of different functional groups in their molecular structure.[7–11] This versatility has allowed the formation of coordinated ylides in different binding modes: C coordinated (via the Cα atom), O bonded (via the carbonyl O), N-bonded (via the N of the cyano group), or even situations in which the same ylide shows a combination of binding modes.[7]

Synthesis of complexes derived from phosphorus ylides and Hg(II) salts was started in 1965 by Nesmeyanov et al.[12] In 1975, Weleski et al.[13] proposed a symmetric halide-bridged dimeric structure for Hg(II) halide complexes, whereas Kalyanasundari et al.[14] reported an asymmetric halide-bridged dimeric structure in 1995. In 1985, Sanehi et al.[15] reported a mononuclear Hg(II) complex of phosphorus ylides without any structural characterization. The α-keto-stabilized phosphorus ylides $R_3PC(R')COR''$ show interesting properties such as high stability and ambidentate character as ligands (C vs. O coordination).[16–19] We have recently focused on the synthesis of binuclear and polynuclear complexes using mercury(II) salts and phosphorus ylides and investigation of their spectroscopic and crystal structures.[20–22] New developments in the crystal chemistry of metal–organic coordination polymers have introduced many novel materials with various structural features and properties. Supramolecular structures with mercury(II) atoms seem to have much similarity with low-valent main group elements than the transition metals, because they form structures with low-coordinate linear or other distorted coordination geometries.[23]

Antibacterial agents are often co-administered with an inhibitor that breaks down the bacterial resistance mechanism and increases the effectiveness of the inhibitor agents[24] The development of compounds with the ability to inhibit bacterial growth has been of great interest in recent years due to the increase of bacterial resistance against present antibiotics and antibacterial compounds[25] Antibacterial agents have potential to be used both in hospital equipment and in everyday items such as soaps, detergents, health, and skincare products and household cleaners[24] Inorganic antibacterial materials have several benefits over commonly used organic compounds, including chemical stability, thermal resistance, safety to the user, long lasting action period, etc.[26]

Herein, we report the self-assembly and resulting structures of a new phosphorus ylide and four mercury (II) complexes of different compositions, $[HgX_2Y]_2$ and $[Hg(NO_3)_2Y]_n$ [X = Cl, Br, and I; Y= $Ph_3PCHC(O)PhCN$]. These compounds have been characterized by Fourier-transform infrared (FT-IR), ^1H nuclear magnetic resonance (NMR), ^{31}P NMR, and ^{13}C NMR spectroscopic studies, and for phosphorus ylide **Y** and the $[Hg(NO_3)_2Y]_n$ complex, additionally, by single-crystal X-ray analysis. Throughout this research, the antibacterial activity of the synthesized ylide and complexes has been studied by the disc diffusion method against specific gram-positive and gram-negative bacteria.[27]

2 | EXPERIMENTAL

2.1 | General considerations

Solvents were reagent grade and starting materials were purchased from commercial sources and used without further purification. Melting points were measured on an SMPI apparatus. IR spectra were recorded on a Perkin Elmer G X FT-IR spectrometer from KBr pellets. ^1H, $^{13}C\{^1H\}$, and $^{31}P\{^1H\}$ NMR spectra were recorded on a 250-/400-MHz Bruker and a 90-MHz JEOL spectrometer using deuterated dimethyl sulfoxide (DMSO-d_6) or $CDCl_3$ as solvents at 25 °C. Chemical shifts (ppm) were reported according to the internal standard tetramethylsilane (^1H, ^{13}C) and external standard 85% phosphoric acid (^{31}P). Coupling constants were given in Hertz. Suitable crystals were obtained by slow evaporation of methanol as the solvent and vapor diffusion of diethyl ether into acetonitrile and mounted in random orientation or mounted on a nylon loop.

2.2 | X-ray crystallography

Colorless crystals of the synthesized phosphorus ylide **Y** and mercury(II) nitrate complex **4** were crystallized by vapor diffusion of diethyl ether into chloroform. A suitable crystal was selected and mounted on a nylon loop on a SuperNova, Dual, Cu at zero, Atlas diffractometer. Using Olex2,[28] the structure was solved with SHELXS.[29] Data were collected for **Y** at 293(2) K with structure solution program using direct methods. For complex **4** the crystal was kept at 100.0(1) K during data collection, which was performed with structure solution program using intrinsic phasing. Both data were refined with the SHELXL[30] refinement package using least-squares minimization on F^2 using all data. All non-hydrogen atoms were refined with anisotropic displacement parameters, whereas all hydrogen atoms were placed at geometrical estimates and refined using the riding model with an isotropic displacement parameter equal to 1.2 times U_{eq} of the parent atom. Both structures showed residual electron density peaks around the metal atoms due to minor disorder, 0.27 and −0.30 e Å^{-3} for **Y**, and 1.82 and −1.28 e Å^{-3} for **4**; attempts to model this disorder were not successful.

2.3 | Synthesis of $Ph_3PCHC(O)PhCN$ (Y)

A solution consisting of triphenyl phosphine (0.26 g, 1 mmol) and 2-bromo-4-cyanoacetophenone (0.22 g, 1 mmol) in dried acetone (25 ml) was stirred at 40 °C for 12 hr. The resulting white precipitate was filtered off, washed with petroleum benzine, and dried. Further treatment with an aqueous solution of NaOH (0.5 M, 10 ml) led to the elimination of HBr, affording the free ligand (**Y**). The resulting white precipitate was filtered off, washed with petroleum benzine, and dried (Scheme 1).[22,31–33]

2.3.1 | Data for $Ph_3PCHC(O)PhCN$ (Y)

Yield: 0.37 g (92%), melting point, 115–117 °C. IR (KBr disk, cm^{-1}) υ: 1572 (C=O), 883 (P–C) (Figure S1). ^1H NMR ($CDCl_3$) δ_H: 4.40 (br, 1H, CH); 7.25–8.03 (m, 19H, Ph) (Figure S2). ^{31}P NMR ($CDCl_3$): δ_P = 16.84 (s, PPh_3) (Figure S3). ^{13}C NMR ($CDCl_3$): δ_C = 52.10 (d, CH, $^1J_{PC}$ = 111.33); 112.43 (s, CN); 119.14–133.40 (m, Ph); 182.30 (s, CO) (Figure S4).

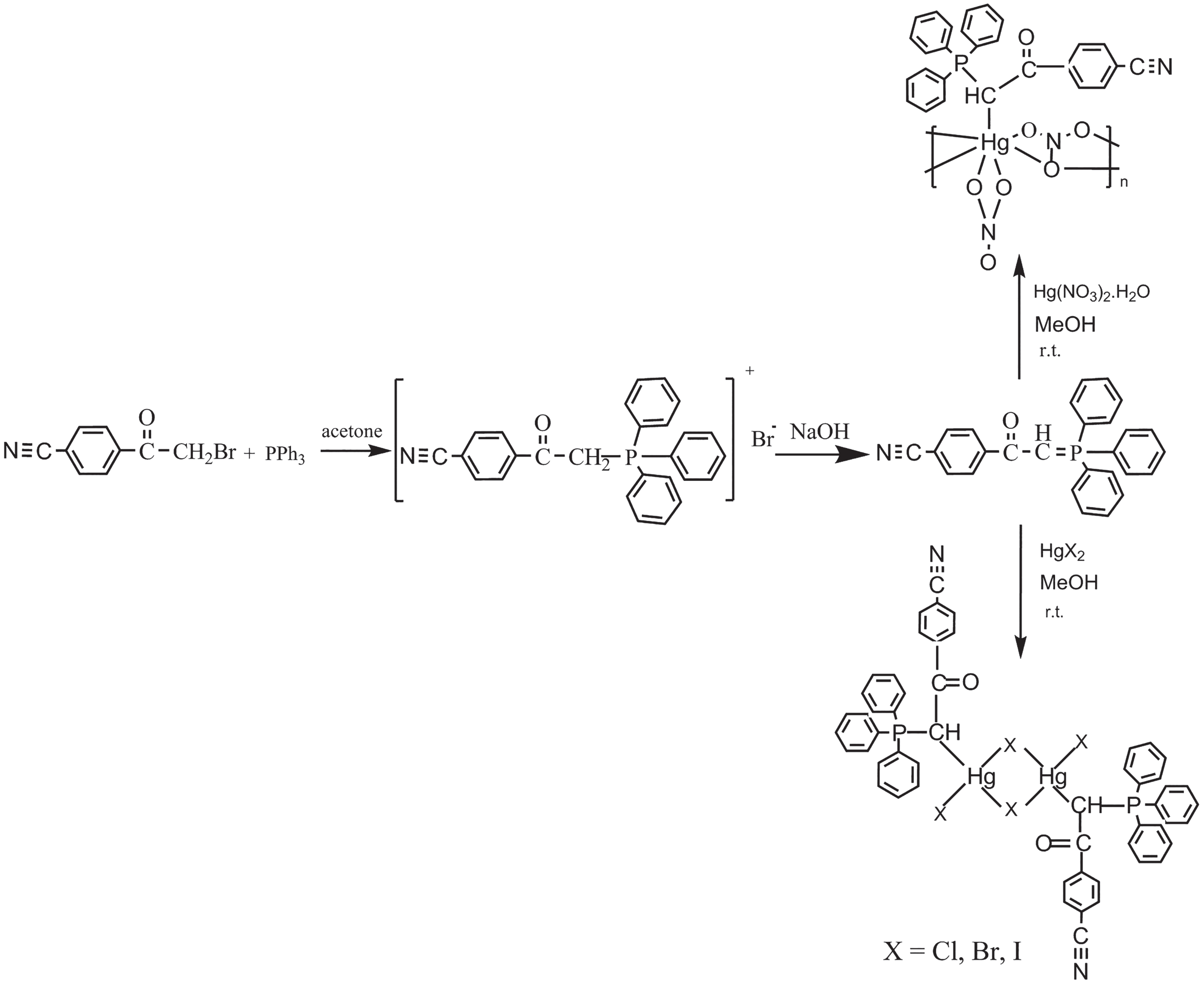

SCHEME 1 Synthesis of the ylide **Y** and its complexes (**1**), (**2**), (**3**), and (**4**). r.t., room temperature

2.4 | Synthesis of Hg(II) halide dimeric complexes

2.4.1 | General procedure

To HgX_2 (1 mmol of 0.26 g $HgCl_2$ or 0.35 g $HgBr_2$ or 0.45 HgI_2) dissolved in 10 ml of dried methanol, the ylide (0.40 g, 1 mmol) was added at room temperature. The mixture was stirred for approximately 8 hr and products were filtered, washed with petroleum benzine, and dried (Scheme 1).[34–36]

2.4.2 | Data for $[Ph_3PCHC(O)PhCN{\cdot}HgCl_2]_2$ (1)

Yield: 0.84 g (65%), decomp. at 192–195 °C. IR (KBr disk, cm^{-1}) υ: 1630 (C=O), 807 (P–C) (Figure S5). ^1H NMR (DMSO-d_6) δ_H: 5.26 (br, 2H, CH); 7.19–8.15 (m, 38H, Ph) (Figure S6).^{31}P NMR (DMSO-d_6): δ_P = 21.01 (s, PPh_3) (Figure S7). ^{13}C NMR (DMSO-d_6): δ_C = 49.07 (d, CH, $^1J_{PC}$ = 84.52); 112.09 (s, CN); 118.66–133.17 (m, Ph); 185.55 (s, CO) (Figure S8).

2.4.3 | Data for $[Ph_3PCHC(O)PhCN{\cdot}HgBr_2]_2$ (2)

Yield: 0.88 g (58%), decomp. at 214–217 °C. IR (KBr disk, cm1) υ: 1641 (C=O), 816 (P–C) (Figure S9). ^1H NMR (DMSO-d_6) δ_H: 5.09 (d, $^2J_{PH}$=12.50 Hz, 2H, CH); 7.59–8.11 (m, 38H, Ph) (Figure S10). ^{31}P NMR (DMSO-d_6): δ_P = 20.03 (s, PPh_3) (Figure S11). ^{13}C NMR (DMSO-d_6): δ_C = 49.17 (d, CH, $^1J_{PC}$ = 94.35); 113.14 (s, CN); 119.16–143.61 (m, Ph); 185.02 (s, CO) (Figure S12).

2.4.4 | Data for $[Ph_3PCHC(O)PhCN{\cdot}HgI_2]_2$ (3)

Yield: 1.17 g (69%), decomp. at 214–217 °C. IR (KBr disk, cm^{-1}) υ: 1637 (C=O), 801 (P–C) (Figure S13). ^1H NMR (DMSO-d_6) δ_H: 4.94 (d, 2H, CH, $^1J_{PC}$ = 20.00); 7.68–8.19 (m, 38H, Ph) (Figure S14). ^{31}P NMR (DMSO-d_6): δ_d = 17.65 (s, PPh^3) (Figure S15). ^{13}C NMR (DMSO-d_6): dC = 50.12 (d, CH, $^1J_{PC}$ = 103.63); 113.65 (s, CN); 119.03–144.12 (m, Ph); 186.93 (s, CO) (Figure S16).

2.5 | Synthesis of the Hg(II) nitrate complex

To $Hg(NO_3)_2{\cdot}H_2O$ (0.36 g, 1 mmol) dissolved in 10 ml of dried methanol, the ylide (0.40 g, 1 mmol) was added at room temperature. The mixture was stirred for about 8 hr and products were filtered, washed with petroleum benzine, and dried (Scheme 1).[37–39]

2.5.1 | Data for $[Ph_3PCHC(O)PhCN{\cdot}Hg(NO_3)_2]_n$ (4)

Yield: 0.69 g (87%), decomp. at 217 °C. IR (KBr, cm^{-1}) υ: 1659 (C=O), 815 (P–C) (Figure S17). ^1H NMR (DMSO-d_6) δ_H: 6.49 (br, 1H, CH); 7.48–8.29 (m, 19H, Ph) (Figure S18). ^{31}P NMR (DMSO-d_6): δ_P = 27.64 (s, PPh^3) (Figure S19). ^{13}C NMR (DMSO-d_6): δ_C = 116.36 (s, CN); 118.29–139.00 (m, Ph); 192.84 (s, 2C, CO) (Figure S20).

2.6 | Computational studies

The geometries of the synthesized mercury(II) halide complexes $[\{Ph_3PCHCOC_6H_4\text{-}p\text{-}CN\}\rightarrow HgX_2]_2$ (X = Cl, Br, I) were optimized without symmetry constraints at the BP86[40]/def2-SVP[41] level of theory using the Gaussian 09[42] optimizer. Recent studies have shown that BP86 is a suitable method for the calculation of L→M bond properties in ylidic complexes.[43,44] A natural bond orbital (NBO) analysis was also carried out with the internal model Gaussian 09 program[45,46] The observed geometry of the already synthesized compound, $[\{Ph_3PCHCOC_{10}H_7\}\rightarrow HgX_2]_2$ (X = Cl, Br, I), was used as a basis for the density functional theory (DFT) calculations.[47] The bonding analyses, in terms of energy-decomposition analysis (EDA), were conducted at the BP86/TZ2P(ZORA)//BP86/def2-SVP level of theory with C1 symmetry. The basis sets for all elements have triple-f quality augmented by one set of polarization functions [ADF basis set TZ2P(ZORA)] with the program package ADF2013.01. EDA calculations were carried out to analyze the nature of the $C_{(carbene)}\rightarrow M$ bond.[48–50]

2.7 | Antibacterial assay

The potential antibacterial effects of the synthesized phosphorus ylide **Y** and mercury(II) complexes **1**–**4** were investigated by the disc diffusion method against five gram-positive bacteria, namely, *Bacillus cereus* (American Type Culture Collection [ATCC] 7064), *Staphylococcus saprophyticus* (ATCC 15305), *Bacillus subtilis* (ATCC 6633), *Staphylococcus aureus* (ATCC 6538), and *Bacillus thuringiensis* (Lio), and against four gram-negative bacteria, namely, *Escherichia coli* (plant tissue and cell culture [PTCC] 10009), *Pseudomonas fluorescens* (PTCC 1181), *Pseudomonas aeruginosa* (ATCC 25923), and *Klebsiella oxytoca* (Lio).[51] The organisms were sub-cultured in nutrient broth and nutrient agar (Oxoid Ltd.) for experimental use, while agar (Diagnostic Sensitivity Test Agar or D.S.T.A.; Oxoid Ltd.) was used in antibiotic sensitivity testing.

The complexes and ligand were dissolved in DMSO to a final concentration of 1 mg ml^{-1} and then sterilized by filtration using a 0.2-μm filter (Millipore). All tests were carried using 10 ml of suspension containing 1.5×10^8 bacteria ml^{-1} and spread on nutrient agar medium. The test samples were dissolved in DMSO at a concentration of 1 mg ml^{-1}. The sensitivity testing was performed using the agar-gel diffusion method.[24,52] In each disk, 20 μl of each chemical, containing 10 μg in DMSO, was loaded. Because DMSO was used as a solvent, it was also screened against all bacterial species used in this study as a negative control. Chloramphenicol was used as a positive reference standard. The diameters of inhibition zones generated by the complexes were measured.

3 | RESULTS AND DISCUSSION

3.1 | Synthesis

The phosphorus ylide **Y** was synthesized by reaction of 2-bromo-4′-cyanoacetophenone with triphenylphosphine and concomitant treatment with NaOH. The mercury complexes were prepared through the reaction of **Y** as a new phosphorus ylide ligand, $Ph_3PCHC(O)PhCN$, and a mercury salt, resulting in the formation of complexes with the general stoichiometry $[HgX_2Y]_2$, where X is chloride, bromide, or iodide. The one-dimensional polymer $[Hg(NO_3)_2(Y)]_n$ (**4**) was also synthesized by the reaction of **Y** and $Hg(NO_3)_2{\cdot}H_2O$ in methanol. In fact, one equivalent of HgX_2 or $Hg(NO_3)_2{\cdot}H_2O$ reacts with one equivalent of **Y** to give a precipitate which proved to consist of mercury complexes and one-dimensional mercury polymer, respectively. The synthesized polymeric $[Hg(NO_3)_2Y]_n$ complex can be recrystallized using a large volume of acetonitrile to provide crystals suitable for X-ray diffraction analysis. The results of the crystal structure determinations of **Y** and **4** are consistent with the chemical and spectroscopic analyses, providing clear evidence of the formation of the phosphorus ylide and the corresponding $[Hg(NO_3)_2Y]_n$ complex.

3.2 | X-ray crystallography

The molecular structures of the synthesized phosphorus ylide **Y** and mercury(II) nitrate complex **4** are shown in Figure 1 and the relevant parameters concerning data collection and refinement are summarized in Table 1. Selected bond distances and bond angles for the unit cells of **Y** and **4** are presented in Tables 2 and 3.

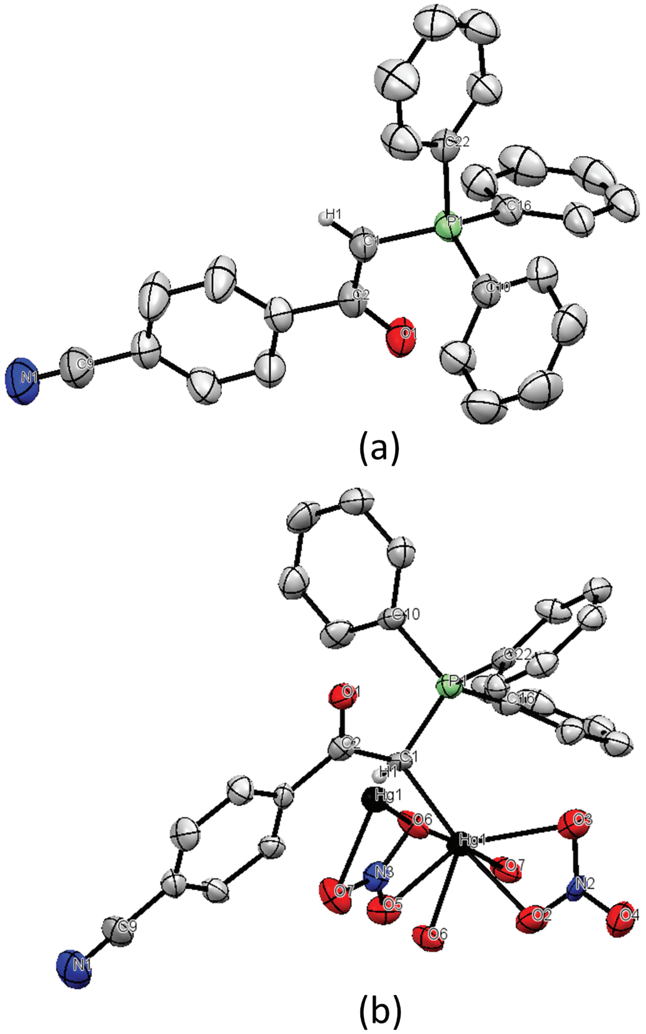

FIGURE 1 (a) X-ray crystal structure of ylide **Y**, $Ph_3PCHC(O)PhCN$, and (b) complex **4**, $[Ph_3PCHC(O)PhCN{\cdot}Hg(NO_3)_2]_n$ asymmetric unit

The X-ray structure of stabilized phosphorus ylide **Y** is shown in Figure 1a. Ylidic resonance is important in **Y** stabilized by electron-withdrawing substituents due to electronic delocalization between the P–C bond, the ylidic bond, and an acyl group.[53,54] There is a slightly distorted tetrahedral arrangement around the P atom, as observed for stabilized keto–ester phosphorus ylides.[55] The P–C bonds [P1–C1 = 1.729(2), P1–C10 = 1.813(3), P1–C16 = 1.809(2) and P1–C22 = 1.809(2) Å] comparable to analogous distances in [55] and [56] are longer than the typical double P–C bond in methylenetriphenylphosphorane and Ph_3PCH_2. The X-ray crystal structure analysis shows that complex **4** adopts a non-centrosymmetric polymeric structure with NO_3 bridge. As illustrated in Figure 1, the Hg atom in each unit surrounded by six oxygen comes from NO_3 groups and ylidic carbon with the Hg–C distance of 2.120(6) Å and two oxygen atoms of the nitrate ligand

TABLE 1 Crystallographic data summary for ylide **Y** and complex **4**

Compound	Ylide Y	Complex 4
Empirical formula	$C_{27}H_{20}NOP$	$C_{29}H_{23}HgN_4O_7P$
Formula weight	405.41	771.07
Temperature (K)	293(2)	100.0(1)
Crystal system	Monoclinic	Orthorhombic
Space group	$P2_1/n$	$P2_12_12_1$
a (Å)	13.2796(2)	10.3387(2)
b (Å)	11.29431(19)	16.1945(4)
c (Å)	14.9318(2)	17.4654(3)
α (°)	90	90
β (°)	106.1325(18)	90
γ (°)	90	90
Volume ($Å^3$)	2151.34(6)	2924.23(10)
Z	4	4
ϱ_{calc} ($g\ cm^{-3}$)	1.252	1.751
μ (mm^{-1})	1.264	5.371
F(000)	848.0	1504.0
Crystal size (mm^3)	0.25 × 0.191 × 0.127	0.327 × 0.192 × 0.144
Radiation	Cu-K_α ($\lambda = 1.54184$)	Mo-K_α ($\lambda = 0.71073$)
2θ range for data collection (°)	7.892 to 150.672	5.03 to 59.382
Index ranges	$-16 \leq h \leq 16, -11 \leq k \leq 13, -18 \leq l \leq 17$	$-13 \leq h \leq 13, -22 \leq k \leq 20, -24 \leq l \leq 21$
Reflections collected	20,646	18,773
Independent reflections	4315 [$R_{int} = 0.0577$, $R_{sigma} = 0.0477$]	7118 [$R_{int} = 0.0592$, $R_{sigma} = 0.0814$]
Data/restraints/parameters	4315/0/271	7118/0/381
Goodness-of-fit on F^2	1.020	1.026
Final *R* indexes [$I \geq 2\sigma$ (I)]	$R_1 = 0.0575$, $wR_2 = 0.1411$	$R_1 = 0.0438$, $wR_2 = 0.0669$
Final *R* indexes [all data]	$R_1 = 0.0842$, $wR_2 = 0.1624$	$R_1 = 0.0605$, $wR_2 = 0.0753$
Largest diffraction peak/hole (e $Å^{-3}$)	0.27/−0.30	1.82/−1.28
Flack parameter		0.491(9)

with Hg–O distances of 2.159(6) and 2.512(7) Å (Table 3). The coordination number in this complex is seven (one of ylide, two of one bidentate nitrate anion, and four of two bridged nitrates). There are only a few inorganic examples of bridging nitrates with different coordination modes: bidentate,[57] tridentate,[58] and tetradentate[59] but in **4** there are two different nitrate anions: one of them acts as bidentate and the other one acts as both bidentate and bridging groups (totally tetradentate). The C2–O1 distance in complex **4** is shorter than the aforementioned ylide, showing the C coordination of ylide to the metal center. By contrast, the P1–C1 distance in complex **4** is longer than ylide, showing the elimination of electron delocalization in P–C1–C2=O by coordination of C1 to the Hg center.

3.3 | Spectroscopy

3.3.1 | Infrared spectra

In the IR spectra of the phosphorus ylide **Y**, a strong stretching absorption due to the carbonyl group was observed at 1572 cm^{-1}.[60,61] Coordination of the ylide through the carbon atom causes an increase in νCO, whereas for O coordination a lowering of νCO is expected. Because of the coordination of **Y** to mercury(II) atoms, the resonance between C=O and C=P is destroyed and C=O becomes weaker. As a result, the infrared spectra of the complexes in the solid state show a νCO in the range of 1630–1659 cm^{-1} at higher frequencies with respect to the free ylide. The νPC frequency, which is also

TABLE 2 Selected key bond lengths (Å) and angles (°) for complex **4**

Bond lengths	Length (Å)
Hg1–O2	2.159(6)
Hg1–O5	2.512(7)
Hg1–C1	2.120(8)
P1–C1	1.800(8)
P1–C10	1.806(9)
P1–C16	1.797(9)
P1–C22	1.803(9)
C1–C2	1.495(4)
O1–C2	1.229(3)
Bond angles	Angle (°)
O2–Hg1–O5	80.7(2)
C1–Hg1–O2	173.1(3)
C1–Hg1–O5	105.0(3)
N2–O2–Hg1	106.8(5)
N3–O5–Hg1	109.4(6)
P1–C1–Hg1	112.3(4)
C2–C1–Hg1	111.0(5)

TABLE 3 Selected key bond lengths (Å) and angles (°) for ylide **Y**

Bond lengths	Length (Å)
P1–C1	1.729(2)
P1–C10	1.813(3)
P1–C16	1.809(2)
P1–C22	1.809(2)
O1–C2	1.252(3)
C1–C2	1.390(3)
Bond angles	Angle (°)
C1–P1–C10	114.35(11)
C1–P1–C16	113.27(11)
C1–P1–C22	107.55(11)
C16–P1–C10	109.09(11)
C16–P1–C22	106.05(11)
C22–P1–C10	105.93(11)
C2–C1–P1	118.73(18)
C11–C10–P1	119.47(18)
C15–C10–P1	120.97(19)
C17–C16–P1	122.2(2)
C21–C16–P1	118.17(19)
C23–C22–P1	121.79(19)
C27–C22–P1	119.27(19)

diagnostic of the coordination, occurs at 883 cm^{-1} for **Y**. In this study, the νPC values for all complexes were shifted to lower frequencies, because P=C is stronger and is observed in the range of 801–816 cm^{-1}.[60,62] According to the spectra, the interaction in the binuclear complexes is weaker than in the polymeric structure (Table 4).

3.3.2 | NMR spectral data

In the ^{1}H NMR spectra, methinic protons exhibit doublet or broad doublet signals. This broadening might be a result of coupling to ^{199}Hg and forming satellites.[63] The expected downfield shifts of ^{1}H signals for the PCH group upon complexation in the case of C coordination were observed in their corresponding spectra (Table 4).[64]

The ^{31}P NMR spectra of all the compounds show all the expected resonances for the proposed structures. The ^{31}P NMR spectrum of phosphorus ylide **Y** shows a singlet at 16.83 ppm, which corresponds to the PPh_3 group. The phosphorus atom of this compound shows an upfield shift compared with that of the parent phosphonium salt, suggesting some electron density increase in the P–C bonds.[46,60] At room temperature, ^{31}P NMR spectra of complexes **1–4** exhibit a singlet around 17 to 27 ppm, which can be assigned to the PPh_3 group. This chemical shift is at a lower field than the one observed for the corresponding free ylide (around 16 ppm), indicating that the coordination of the ylide has occurred (Table 4).

The most interesting aspect of the ^{13}C NMR spectra of the complexes is the upfield shift of the signals due to the ylidic carbon. Such an upfield shift of δ 3–10 ppm with reference to the parent ylide was also observed in the case of $[Ph_3PCHC(O)PhCN{\cdot}HgI_2]_2$[65] and our previously synthesized complexes.[66] The ^{13}C shifts of the CO group in the complexes are around 190 ppm, relative to 182 ppm noted for the same carbon in the parent ylide, confirming the correct synthesis of these complexes.

3.4 | Theoretical studies

The structures of synthesized mercury(II) halide complexes $[\{Ph_3PCHCOC_6H_4\text{-}p\text{-}CN\}{\rightarrow}HgX_2]_2$ [X = Cl (**1**), Br (**2**), I (**3**)] complexes are optimized at the BP86/def2-SVP level of theory. These optimized structures and the trends for the variation of the corresponding bond lengths and bond angles are shown in Figure 2. As can be seen in Figure 2, there is an increasing trend for C→M bond lengths when the Hg_2X_2 fragment changes from Hg_2Cl_2 to Hg_2I_2 as $Hg_2I_2 > Hg_2Br_2 > Hg_2Cl_2$ for $[\{Ph_3PCHCOC_6H_4\text{-}p\text{-}CN\}{\rightarrow}HgX_2]_2$ [X = Cl (**1**), Br (**2**), I (**3**)] complexes.

TABLE 4 FT-IR, ^{13}C, and ^{1}H and ^{31}P NMR data of the ylide and its synthesized complexes

Compounds	FT-IR		^{1}H NMR		^{31}P NMR	^{13}C NMR		
	νCO	νPC	δCH	J(P–H)	δPCH	δCO	δCH	J(P–CH)
Y[a]	1572	883	4.40(br)	–	16.84(s)	182.30(s)	52.10(d)	111.33
1[b]	1630	807	5.26(br)	–	21.01(s)	185.55(s)	49.07(d)	84.52
2[b]	1641	816	5.09(d)	12.50	20.03(s)	185.02(s)	49.17(d)	94.35
3[b]	1637	801	4.94(d)	20.00	17.65(s)	186.93(s)	50.12(d)	103.63
4[b]	1659	815	6.49(br)	–	27.64(s)	192.84(s)	–	–

FT-IR, Fourier-transform infrared; NMR, nuclear magnetic resonance; s, Singlet; d, doublet; br, broad.

[a] Record in $CDCl_3$.

[b] Recorded in deuterated dimethyl sulfoxide (DMSO-d_6).

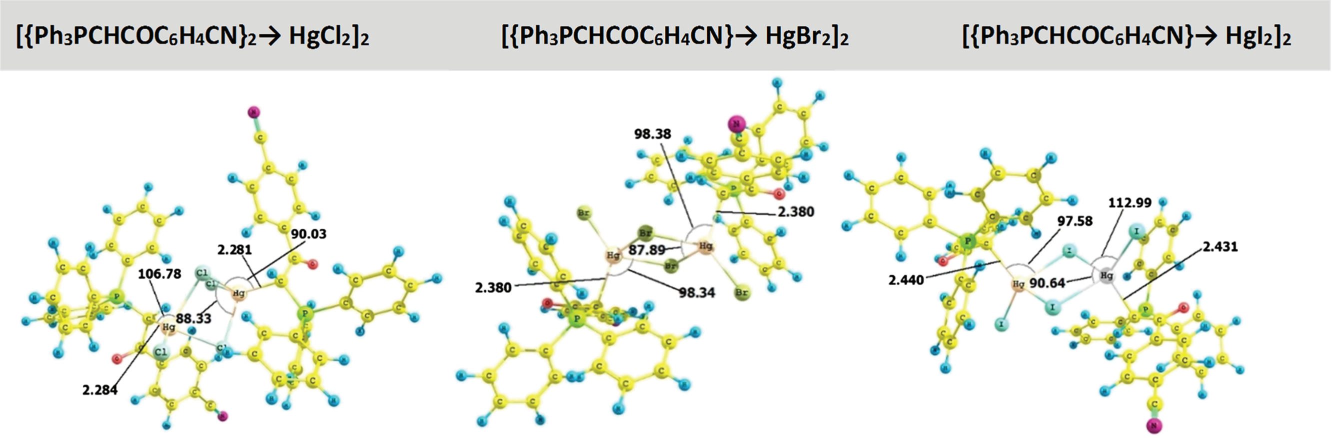

FIGURE 2 Optimized structures of [{$Ph_3PCHCOC_5H_4CN$}$_2$→HgX_2]$_2$ (X = Cl, Br, I) complexes at the BP86/def2-SVP level of theory. Bond lengths are given in Angstrom, bond angles in degrees

This trend is predictable due to the change in halogen electronegativity and the halogen atomic radius.

In this regard, the largest (2.43 Å) and the shortest (2.28 Å) C→M bond lengths are related to the [{$Ph_3PCHCOC_5H_4CN$}→HgI] (**3**) and [{$Ph_3PCHCOC_5H_4CN$}→HgCl] (**1**) complexes, respectively. These data are in good agreement with the calculated interaction energies (ΔE_{int}) for all of these complexes. The ΔE_{int} between the studied phosphorus ylide {$Ph_3PCHCOC_6H_4CN$} and Hg_2X_2 [X= Cl (**1**), Br (**2**), I (**3**)] fragments in the optimized structures of [{$Ph_3PCHCOC_6H_4CN$}→HgX_2]$_2$ [X = Cl (**1**), Br (**2**), I (**3**)] were calculated at the BP86/def2-SVP level of theory according to the following equation:

$$\Delta E_{int} = E_{AB} - \left(E^{A}_{AB} + E^{B}_{AB}\right) \qquad (1)$$

where E^{A}_{AB} stands for the electronic energy of the phosphorus ylide fragments and E^{B}_{AB} represents the electronic energy of the Hg_2X_2 [X= Cl(**1**), Br(**2**), I(**3**)] fragments in the optimized structures [{$Ph_3PCHCOC_6H_4CN$}→HgX_2]$_2$ [X = Cl (**1**), Br (**2**), I (**3**)].

The interaction energies (ΔE_{int}) between the ylidic part of all complexes and Hg_2X_2 fragment (X = Cl, Br, I) are illustrated in Table 5. The results show that the C→M bond interaction energies are very strong and decrease by changing the X atom from Cl to I in the phosphorus ylide complexes in the following order: Cl > Br > I. These results show that with decreasing electronegativity and S character of carbon, there is a decrease in interaction energy.

Regarding ΔE_{int}, the [{$Ph_3PCHCOC_6H_4CN$}→HgCl] (**1**) and [{$Ph_3PCHCOC_6H_4CN$}→HgI] (**3**) complexes have the

TABLE 5 ΔE_{int} (kcal mol^{-1}) for [{$Ph_3PCHCOC_6H_4CN$}$_2$→HgX_2]$_2$ (X = Cl, Br, I)

Complex	ΔE_{int}
[{$Ph_3PCHCOC_6H_4CN$}→$HgCl_2$]$_2$	−135.33
[{$Ph_3PCHCOC_6H_4CN$}→$HgBr_2$]$_2$	−68.66
[{$Ph_3PCHCOC_5H_4CN$}→HgI_2]$_2$	−55.16

highest (–135.33 kcal mol^{-1}) and the lowest (–55.16 kcal mol^{-1}) amount of interaction energies, respectively. Larger interaction energies lead to a strong bond and respective short C→M bond length (Table 5).

Further investigation about C→M bonding interaction is performed using the NBO analysis. This method gives a more accurate and quantitative determination about C→M bonding interaction. The partial charge values of the $C_{(ylidic)}$, Hg atom, and Hg_2X_4 fragment [X = Cl (**1**), Br (**2**), I (**3**)] are illustrated in Table 6. Concerning $[\{Ph_3PCHCOC_6H_4CN\}\rightarrow HgX]$ [X = Cl (**1**), Br (**2**), I (**3**)] complexes, the $C_{(ylidic)}$ and Hg fragment in complexes carry negative and positive charges, respectively.

A comparison of the Wiberg bond indices (WBIs) for C→Hg bonds in $[\{Ph_3PCHCOC_6H_4CN\}\rightarrow HgX_2]_2$ [X = Cl (**1**), Br (**2**), I (**3**)] complexes is provided in Table 6. The highest value of WBI (0.40) for C→Hg bonds is related to the $[\{Ph_3PCHCOC_6H_4CN\}\rightarrow HgCl_2]_2$ (**1**) complex.

EDA is a suitable method to characterize the ionic and covalent share of a distinct bond in a complex (Table 7). The bonding analysis in terms of EDA of all the aforementioned complexes was carried out at the BP86/TZ2P(ZORA)//BP86/def2-SVP level of theory with C1 symmetry using the program package ADF2013.01.

In the EDA calculation, ΔE_{int} consists of four main parameters, which are illustrated in the following equation:

$$\Delta E_{\text{int}} = \Delta E_{\text{elstat}} + \Delta E_{\text{Pauli}} + \Delta E_{\text{orb}} + \Delta E_{\text{disp}} \qquad (2)$$

where ΔE_{elstat} is electrostatic interaction, ΔE_{Pauli} is Pauli repulsion, ΔE_{orb} is orbital interaction, and ΔE_{disp} is dispersion energy between two fragments. Table 7 presents the results of the EDA for all the aforementioned complexes.

The strength and nature of donor–acceptor bonds (C→M) of the two-electron donor phosphorus $\{Ph_3PCHCOC_6H_4CN\}$ ylide with HgX_2 [X = Cl (**1**), Br (**2**), I (**3**)] were compared. According to Table 6, C→M bond interaction energies are very strong and they are decreased by changing the X atom from Cl to I in phosphorus ylide complexes in the following order: Cl > Br > I, respectively. This trend is predictable due to the change in halogen electronegativity.

The interaction energies calculated from EDA are in good agreement with those extracted from the aforementioned single-point analysis, which also demonstrated Cl > Br > I. Regarding equation (2), the more important factor in interaction energies (ΔE_{int}) in these complexes is electrostatic interaction (ΔE_{elstat}) of about 49%–53%. This share is about 32%–35% for orbital interactions. The larger amounts of ΔE_{elstat} are related to $[\{Ph_3PCHCOC_6H_4CN\}\rightarrow HgCl]$ complexes in the following order: $[\{Ph_3PCHCOC_6H_4CN\}\rightarrow HgCl] > [\{Ph_3PCHCOC_6H_4CN\}\text{-}HgBr] > [\{Ph_3PCHCOC_6H_4CN\}\rightarrow HgI]$ (Table 7).

With respect to the EDA–NOCV method, individual contributions of pairwise interactions are possible. The most important ones are illustrated in Figure 3. The four NOCV pairs regarding the $[\{Ph_3PCHCOC_6H_4CN\}\rightarrow HgX_2]_2$ complexes account for an average of 77% of ΔE_{orb}.

The shapes of orbital pairs Δρ between the donor orbital of ylide and the acceptor part of the Hg_2X_2 fragments are shown in Figure 3. As can be seen, the σ

TABLE 6 Wiberg bond indices (WBIs) of the C–M bond and natural charges of C and M atoms and MR′

Complex	WBI	Hg	$C_{(carbene)}$	Hg_2X_2
$[\{Ph_3PCHCOC_6H_4CN\}\rightarrow HgCl_2]_2$	0.40	0.71	–1.02	–0.48
$[\{Ph_3PCHCOC_6H_4CN\}\rightarrow HgBr_2]_2$	0.36	0.59	–1.00	–0.50
$[\{Ph_3PCHCOC_6H_4CN\}\rightarrow HgI_2]_2$	0.34	0.38	–0.98	–0.52

Fragment in $[\{Ph_3PCHCOC_6H_4CN\}_2\rightarrow HgX_2]_2$ (X = Cl, Br, I) at the BP86/def2-SVP level of theory. Data in parentheses are related to the second carbon in the complexes.

TABLE 7 EDA analysis [BP86/TZ2P(ZORA)//BP86/def2-SVP] of $[\{Ph_3PCHCOC_6H_4CN\}_2\rightarrow HgX_2]_2$ (X = Cl, Br, I) complexes with the C1 symmetry

Complex name	ΔE_{int}	ΔE_{Pauli}	ΔE_{elstat}	ΔE_{orb}	ΔE_{disp}	$\Delta E_{\text{orb},\sigma d}$	$\Delta E_{\text{orb},\sigma d}$	$\Delta E_{\text{orb},\sigma bd}$	$\Delta E_{\text{orb},\sigma bd}$
$[\{Ph_3PCHCOC_5H_4CN\}\rightarrow HgCl_2]_2$	–135.82	253.00	–207.53 (53.30)	–134.55 (34.50)	–47.40 (12.17)	–46.73	–44.38	–6.47	–6.50
$[\{Ph_3PCHCOC_5H_4CN\}\rightarrow HgBr_2]_2$	–112.75	198.64	–159.39 (51.18)	–103.27 (33.20)	–48.72 (15.64)	–35.56	–34.01	–4.94	–4.81
$[\{Ph_3PCHCOC_5H_4CN\}\rightarrow HgI_2]_2$	–102.33	179.08	–138.42 (49.20)	–90.59 (32.19)	–52.39 (18.61)	–31.71	–30.45	–4.17	–3.89

Data in parentheses are the number in percentage.

EDA, energy-decomposition analysis; ΔE_{disp}, dispersion energy between two fragments; ΔE_{elstat}, electrostatic interaction; ΔE_{int}, interaction energies; ΔE_{orb}, orbital interaction; ΔE_{Pauli}, Pauli repulsion; $\Delta E_{\text{orb},\sigma d}$, orbital interaction, σ-donation; $\Delta E_{\text{orb},\sigma bd}$, orbital interaction, σ-back donation.

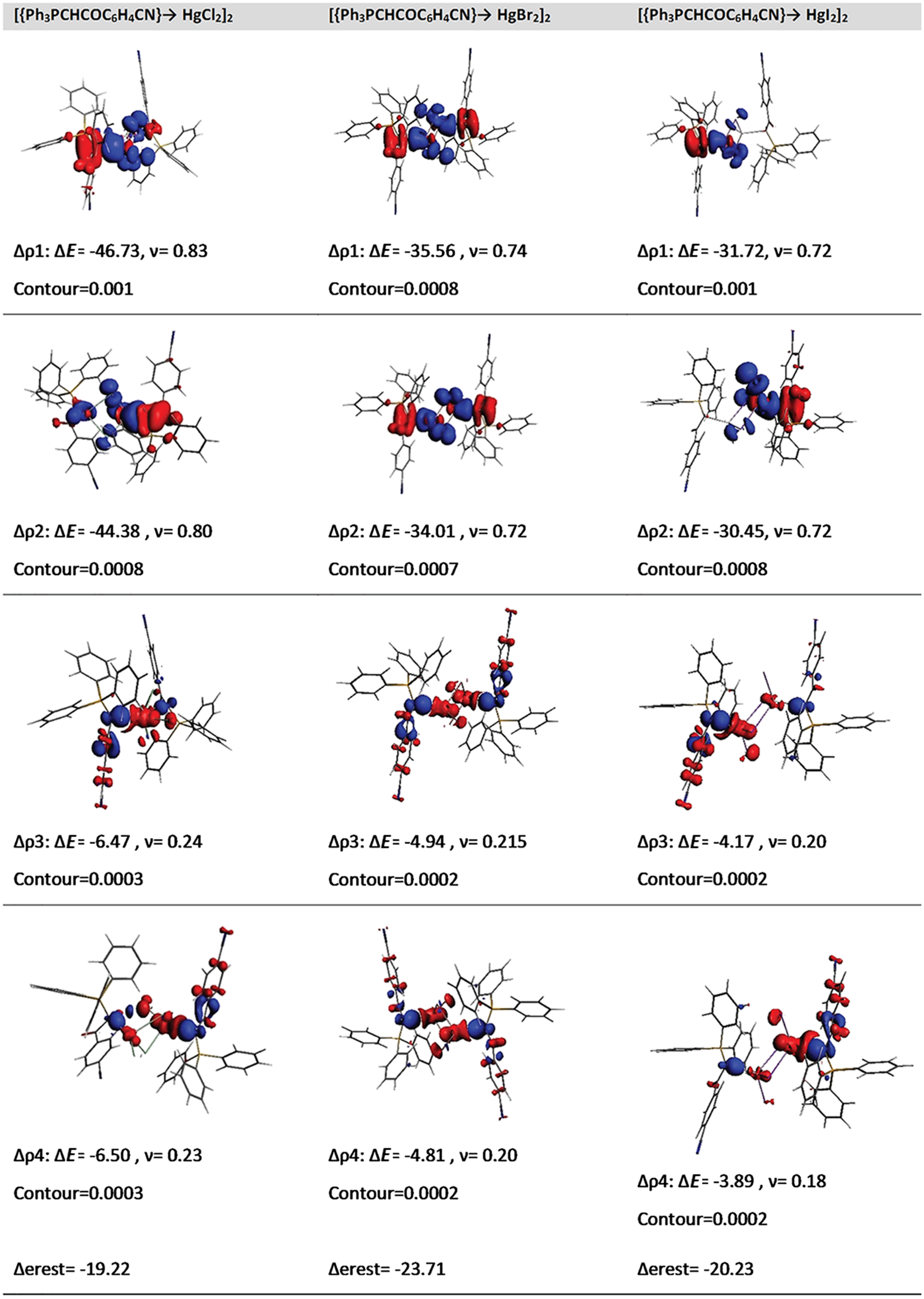

FIGURE 3 Deformation densities associated with the most important orbital interactions $[\{Ph_3PCHCOC_6H_4CN\}_2 \rightarrow HgX_2]_2$ (X = Cl, Br, I) at the BP86/def2-SVP level of theory

donation related to Δρ1 and Δρ2 is the dominant term in ΔE_{orb} and the σ back donation related to Δρ3 and Δρ4 has only a minor effect on ΔE_{orb}. It is thus clear that there is no important π interaction in these complexes.

3.5 | Antibacterial study

The antibacterial activity using the agar disc diffusion method was determined for the synthesized phosphorus ylide **Y** and mercury(II) complexes **1–4**. The results of

TABLE 8 Antibacterial activity of the ylide **Y** and its synthesized complexes **1–4**

	Compounds	**Prevention area**					
	Microorganisms	**Y**	**1**	**2**	**3**	**4**	**Control**
Gram negative	*Escherichia coli*	NA	15	15	17	17	NA
	Pseudomonas fluorescens	NA	22	22	20	18	NA
	Klebsiella oxytoca	18	19	18	18	16	NA
	Pseudomonas aeruginosa	7	16	20	NA	NA	NA
Gram positive	*Bacillus thuringiensis*	NA	21	20	20	17	NA
	Bacillus cereus	NA	35	25	26	21	NA
	Staphylococcus aureus	NA	38	25	26	40	NA
	Staphylococcus saprophyticus	NA	40	25	28	40	NA
	Bacillus subtilis	NA	18	20	18	50	NA

NA, not applicable.

the antibacterial assessments, together with negative and positive controls, are presented in Table 8. In this research, the free ligand and especially the complexes show good antibacterial activity against the bacteria tested, in particular against gram-positive bacteria.

The most effective compounds were $HgCl_2$ and $Hg(NO_3)_2$ complexes (**1** and **4)** against *S. saprophyticus* and *S. aureus* (40-mm inhibition zone). Mercury(II) nitrate complex **4** showed the highest antibacterial activity against *B. subtilis* (50 mm). Inhibition zones of the compounds against *S. saprophyticus* and *S. aureus* were significantly larger than those of chloramphenicol (25 and 27 mm). These compounds also showed a wide inhibition zone at a very low concentration. The lowest inhibition zone was observed for the phosphorus ylide **Y** (7 mm) against *P. aeruginosa* and *K. oxytoca* (18 mm). This ligand did not show any antibacterial effect and inhibition zones against all the other studied bacterial strains. However, the synergistic or antagonistic effect of one compound, present in minor percentage of a mixture, has to be considered as well.[67,68] The antibacterial activity can also be influenced by the slow release of the ligands inside the bacterial cell. We can consider that different coordination modes of the ligands to the metal complex may facilitate the ability of a metal complex to cross the lipid layer of the bacterial cell membrane and in this way may affect the mechanisms of growth and development of bacteria.[69] A comparative study of the growth inhibition zone values of the phosphorus ylide **Y** and mercury(II) complexes **1–4** indicates that the complexes exhibit clearly higher antibacterial activity than the free ligand **Y**. With antibacterial activities of samples compared with those of a reference antibiotic (chloramphenicol), it seems that all complexes have remarkable inhibitory potencies against bacterial species considered in this research (Table 8). Although all bacteria tested are sensitive to chloramphenicol, the antibacterial effects of some complexes, especially $HgCl_2$ and $Hg(NO_3)_2$ complexes **1** and **4**, were higher than these antibiotics. These results indicate that the complexes studied may be used in the treatment of diseases caused by the bacteria tested. However, further studies are needed to evaluate the in vivo potential of these compounds in animal models.

4 | CONCLUSIONS

The synthesis and characterization of organic/inorganic composite polymer and binuclear Hg(II) complexes of a new α-keto-stabilized phosphorus ylide are described. On the basis of the physicochemical and spectroscopic data, we propose that the ligand herein exhibits monodentate C coordination to the metal center, which is confirmed by the X-ray crystal structure of the polymeric mercury(II) nitrate complex **4** and theoretical study. The electronic and molecular structure of mercury(II) halide complexes **1–3** have been studied by DFT at the BP86/def2-SVP level of theory. The nature of the C–Hg bond in complexes **1–3** was investigated using the NBO and EDA methods. The results confirm that electrostatic interactions are the major interactions among EDA components at about 49%–53% while the share of orbital interactions is about 32%–35% of total interaction energies. In addition, the antibacterial studies of these compounds demonstrate that a group of antimicrobial agents with potential application for the control of bacterial infections might be helpful in preventing the progress of various infections and can be used as alternative systems for medicines.

ORCID

Seyyed Javad Sabounchei https://orcid.org/0000-0001-9000-5304

REFERENCES

[1] G. W. Ylid Chemistry, V. A. W. Johnson, *Organic Chemistry, Vol. 7*, Vol. 79, Academic Press, Inc., New York-London1966.

1. Aufl., X, 388 S., zahlr. Abb., geb. $12.50. *Angewandte Chemie* **1967** 832.

[2] JIG. Cadogan. Organophosphorus reagents in organic synthesis: Academic Pr; **1979**.

[3] R. Engel, *Synthesis of Carbon-Phosphorus bonds*, CRC Press, Boca Raton, FL **1988**.

[4] H. Hudson. Nucleophilic Reactions of Phosphines, ch. 11 in The Chemistry of Organophosphorus Compounds, Primary, Secondary, and Tertiary Phosphates and Heterocyclic Organophosphorus III Compounds. **1990**.

[5] G. Wittig, *Science* **1980**, *210*, 600.

[6] D. Cobridge, *Studies in Inorganic Chemistry* **1995**, *20*.

[7] R. Navarro, E. P. Urriolabeitia, *J. Chem. Soc., Dalton Trans.* **1999**, 4111.

[8] A. W. Johnson, *Ylides and imines of phosphorus*, Wiley-Interscience **1993**.

[9] O. I. Kolodiazhnyi, *Phosphorus Ylides*: *Chemistry and Applications in Organic Synthesis*, John Wiley & Sons, XXXX **2008**.

[10] R. Bertani, M. Casarin, P. Ganis, C. Maccato, L. Pandolfo, A. Venzo, A. Vittadini, L. Zanotto, *Organometallics* **2000**, *19*, 1373.

[11] R. Bertani, L. Pandolfo, L. Zanotto, *Inorg. Chim. Acta* **2002**, *330*, 213.

[12] N. A. Nesmeyanov, V. Novikov, O. Reutov, *J. Organomet. Chem.* **1965**, *4*, 202.

[13] E. T. Weleski Jr., J. L. Silver, M. D. Jansson, J. L. Burmeister, *Sulfonium and Pyridinium Ylids. Journal of Organometallic Chemistry* **1975**, *102*, 365.

[14] M. Kalyanasundari, K. Panchanatheswaran, W. T. Robinson, H. Wen, *J. Organomet. Chem.* **1995**, *491*, 103.

[15] R. Sanehi, R. Bansal, R. Mehrotra. Preparation & Characterisation of Some New Bisphosphonium Ylides & Their Palladium (II) & Mercury (II) Complexes. **1985**.

[16] J. Vicente, M. T. Chicote, J. A. Cayuelas, J. Fernandez-Baeza, P. G. Jones, G. M. Sheldrick, P. Espinet, *J. Chem. Soc., Dalton Trans.* **1985**, 1163.

[17] L. R. Falvello, S. Fernández, R. Navarro, I. Pascual, E. P. Urriolabeitia, *J. Chem. Soc., Dalton Trans.* **1997**, 763.

[18] J. A. Albanese, A. L. Rheingold, J. L. Burmeister, *Inorg. Chim. Acta* **1988**, *150*, 213.

[19] J. Vicente, M. T. Chicote, J. Fernandez-Baeza, *J. Organomet. Chem.* **1989**, *364*, 407.

[20] S. J. Sabounchei, H. Nemattalab, H. R. Khavasi, *J. Organomet. Chem.* **2007**, *692*, 5440.

[21] S. J. Sabounchei, A. Dadrass, M. Jafarzadeh, S. Salehzadeh, H. R. Khavasi, *J. Organomet. Chem.* **2007**, *692*, 2500.

[22] S. J. Sabounchei, V. Jodaian, H. R. Khavasi, *Polyhedron* **2007**, *26*, 2845.

[23] M. A. Pitt, D. W. Johnson, *Chem. Soc. Rev.* **2007**, *36*, 1441.

[24] A. Chehregani, F. Mohsenzadeh, N. Mirazi, S. Hajisadeghian, Z. Baghali, *Pharmaceutical Biology* **2010**, *48*, 1280.

[25] M. Khan, A. Omoloso, *Fitoterapia* **2003**, *74*, 695.

[26] B. Li, *J. Miner. Mater. Charact. Eng.* **2002**, *1*, 61.

[27] M. F. Nejad, M. R. T. B. Olyai, H. R. Khavasi, *Structures* **2010**, *225*, 717.

[28] O. V. Dolomanov, L. J. Bourhis, R. J. Gildea, J. A. Howard, H. Puschmann, *J. Appl. Crystallogr.* **2009**, *42*, 339.

[29] G. M. S. H. E. L. X. T. Sheldrick, *Acta Crystallogr., Sect. A: Found. Adv* **2014**, *70*, C1437.

[30] G. M. Sheldrick, *Acta Crystallographica Section C: Structural Chemistry* **2015**, *71*, 3.

[31] R. Moritz, M. Wagner, D. Schollmeyer, M. Baumgarten, K. Müllen, *Chemistry–a European Journal* **2015**, *21*, 9119.

[32] S. J. Sabounchei, H. Nemattalab, S. Salehzadeh, M. Bayat, H. R. Khavasi, H. Adams, *J. Organomet. Chem.* **2008**, *693*, 1975.

[33] K. Zeka, RR. Arroo, D. Hasa, KJ. Beresford, KC. Ruparelia. New resveratrol analogues for potential use in diabetes and cancer. **2018**.

[34] S. J. Sabounchei, A. Dadrass, F. Akhlaghi, Z. B. Nojini, H. R. Khavasi, *Polyhedron* **2008**, *27*, 1963.

[35] S. J. Sabounchei, M. Zamanian, M. Pourshahbaz, M. Bayat, R. Karamian, M. Asadbegy, *J. Chem. Res.* **2016**, *40*, 130.

[36] S. Samiee, Z. Mahdavifar, A. Azadmanesh, F. Jalilian, M. N. Rahbari, *J. Mol. Liq.* **2016**, *219*, 579.

[37] S. J. Sabounchei, M. S. Hashemi, R. Karamian, S. H. Moazzami Farida, P. Gohari Derakhshandeh, R. W. Gable, K. Van Hecke, *J. Coord. Chem.* **2018**, *71*, 3277.

[38] S. J. Sabounchei, M. Ahmadianpoor, A. Hashemi, F. Mohsenzadeh, R. W. Gable, *Inorg. Chim. Acta* **2017**, *458*, 77.

[39] S. Samiee, L. Shirali. Synthesis, Characterization and Theoretical Studies of New P, C-chelated Mercury (II) Complexes Including Non-Symmetric Phosphorus Ylide. **2015**.

[40] A. D. Becke, *Physical Review a* **1988**, *38*, 3098.

[41] J. P. Perdew, *Phys. Rev. B* **1986**, *33*, 8822.

[42] Gaussian09 RA. 1, MJ Frisch, GW Trucks, HB Schlegel, GE Scuseria, MA Robb, JR Cheeseman, G. Scalmani, V. Barone, B. Mennucci, GA Petersson H. Nakatsuji, M. Caricato, X. Li, H. P. Hratchian, A. F. Izmaylov, J. Bloino, G. Zheng, J. L. Sonnenberg, M. Hada, M. Ehara, K. Toyota, R. Fukuda, J. Hasegawa, M. Ishida, T. Nakajima, Y. Honda, O. Kitao, H. Nakai, T. Vreven, J. A. Montgomery, Jr., J. E. Peralta, F. Ogliaro, M. Bearpark, J. J. Heyd, E. Brothers, K. N. Kudin, V. N. Staroverov, R. Kobayashi, J. Normand, K. Raghavachari, A. Rendell, J. C. Burant, S. S. Iyengar, J. Tomasi, M. Cossi, N. Rega, J. M. Millam, M. Klene, J. E. Knox, J. B. Cross, V. Bakken, C. Adamo, J. Jaramillo, R. Gomperts, R. E. Stratmann, O. Yazyev, A. J. Austin, R. Cammi, C. Pomelli, J. W. Ochterski, R. L. Martin, K. Morokuma, V. G. Zakrzewski, G. A. Voth, P. Salvador, J. J. Dannenberg, S. Dapprich, A. D. Daniels, Ö. Farkas, J. B. Foresman, J. V. Ortiz, J. Cioslowski, and D. J. Fox, Gaussian. *Inc.,* Wallingford CT **2009**, 121:150-166.

[43] M. Sayadi, S. J. Sabounchei, A. Sedghi, M. Bayat, L. Hosseinzadeh, R. W. Gable, *Polyhedron* **2019**, *161*, 179.

[44] S. J. Sabounchei, A. Sedghi, M. Bayat, M. Hosseinzadeh, A. Hashemi, A. Yousefi, R. W. Gable, *J. Mol. Struct.* **2019**, *1175*, 346.

[45] N. K. Nkungli, J. N. Ghogomu, L. N. Nogheu, S. R. D. F. T. Gadre, *Chemistry* **2015**, *3*, 29.

[46] G. M. Sheldrick, *Acta Crystallogr., Sect. A: Found. Crystallogr.* **2008**, *64*, 112.

[47] S. J. Sabounchei, V. Jodaian, H. Nemattalab, *S. Afr. J. Chem.* **2009**, *62*, 9.

[48] A. Schäfer, C. Huber, R. Ahlrichs, *The Journal of Chemical Physics* **1994**, *100*, 5829.

[49] M. Bayat, A. Sedghi, L. Ebrahimkhani, S. J. Sabounchei, *Dalton Transactions* **2017**, *46*, 207.

[50] A. Sedghi, M. Bayat, S. J. Sabounchei, M. Khodabandehloo, *Polyhedron* **2019**, *157*, 208.

[51] A. Bauer, W. Kirby, J. C. Sherris, M. Turck, *Am. J. Clin. Pathol.* **1966**, *45*, 493.

[52] A. D. Russell, J. R. Furr, *J. Appl. Bacteriol.* **1977**, *43*, 253.

[53] F. Castañeda, C. A. Terraza, C. A. Bunton, N. D. Gillitt, M. T. Garland, *Phosphorus, Sulfur, and Silicon* **2003**, *178*, 1973.

[54] F. Castañeda, C. A. Terraza, M. T. Garland, C. A. Bunton, R. Baggio, *Communications* **2001**, *57*, 180.

[55] S. J. Sabounchei, A. Dadras, M. Jafarzadeh, H. R. Khavasi, *Acta Crystallogr., Sect. E: Struct. Rep. Online* **2007**, *63*, o3160.

[56] M. Kalyanasundari, K. Panchanatheswaran, V. Parthasarathi, W. Robinson, H. Wen, *Communications* **1994**, *50*, 1738.

[57] Y. Zhang, L. K. Thompson, J. N. Bridson, M. Bubenik, *Inorg. Chem.* **1995**, *34*, 5870.

[58] B. Neumüller, F. Weller, F. Schmock, K. Dehnicke, *Zeitschrift für Anorganische Und Allgemeine Chemie* **2005**, *631*, 1767.

[59] M. Rafizadeh, V. Amani, M. Broushaky, *Analytical Sciences: X-Ray Structure Analysis Online* **2006**, *22*, x213.

[60] A. Spannenberg, W. Baumann, U. Rosenthal, *Organometallics* **2000**, *19*, 3991.

[61] S. M. Sbovata, A. Tassan, G. Facchin, *Inorg. Chim. Acta* **2008**, *361*, 3177.

[62] J. Vicente, M.-T. Chicote, M.-C. Lagunas, P. G. Jones, *J. Chem. Soc., Dalton Trans.* **1991**, 2579.

[63] J. A. Teagle, J. L. Burmeister, *Inorg. Chim. Acta* **1986**, *118*, 65.

[64] R. Uson, J. Fornies, R. Navarro, P. Espinet, C. Mendivil, *J. Organomet. Chem.* **1985**, *290*, 125.

[65] G. Facchin, R. Bertani, M. Calligaris, G. Nardin, M. Mari, *J. Chem. Soc., Dalton Trans.* **1987**, 1381.

[66] N. L. Holy, N. C. Baenziger, R. M. Flynn, D. C. Swenson, *J. Am. Chem. Soc.* **1976**, *98*, 7823.

[67] J. Gray, P. Norton, R. Alnouno, C. Marolda, M. Valvano, K. Griffiths, *Biomaterials* **2003**, *24*, 2759.

[68] S. Burt, *International Journal of Food Microbiology* **2004**, *94*, 223.

[69] M. Tümer, D. Ekinci, F. Tümer, A. Bulut, *Spectrochim. Acta, Part a* **2007**, *67*, 916.

SUPPORTING INFORMATION

Additional supporting information may be found online in the Supporting Information section at the end of the article.

How to cite this article: Sabounchei SJ, Kazemi Andalib F, Hosseinzadeh M, et al. Binuclear and polymeric Hg(II) complexes of an ambidentate phosphorus ylide: Synthesis, crystal structure, antibacterial activity, and theoretical studies. *Appl Organometal Chem*. 2019;e5265. https://doi.org/10.1002/aoc.5265